

## CHAPTER III



## THEORY

In order to properly investigate on the optimization of WAG process, many related topics have to be considered, for instance, the overview of WAG process, reservoir simulation theory, relative permeability hysteresis model, and parametric study. These topics are thoroughly discussed in detail in this chapter.

### 3.1 WAG process overview

Water alternating gas (WAG) injection has been successfully applied in most field trials since the early 1960's. Most of the fields are located in Canada, USA, and the former Soviet Union. Immiscible and miscible WAG processes have been conducted with different types of injected gas.

The first field trial found in the literature is North Pembina field Alberta, Canada, starting in 1957. Table 3.1 presents all the field cases with description of rock and injected gas types. It is seen that many fluid were selected as an injectant. Miscible displacement was achieved in most of field cases.

Estimated improved oil recovery of WAG field cases over waterflooding is shown in Table 3.2. Type of injection gas was also compared. WAG process with injected CO<sub>2</sub> shows an average improved oil recovery of 10%, while WAG process with injected hydrocarbon gas and nitrogen produce an improved oil recovery of 8%. It is seen that most of the field cases have different injection strategy in term of water-gas ratio and slug size.

Table 3.1: Summary of WAG field cases. (Data from Christensen *et al.* SPE International., Mar. 1998.)

Start up	Name	location	injectant	Type of displacement	Formation
1957	North Pembina	Canada, Alberta	Hydrocarbon	Miscible	Sandstone
1958	Romashikoya	Russia	-	-	-
1960	Liniversity	Texas	LPG	Immiscible	Limestone
1960	Midland Farm	Texas	Propane	Miscible	Limestone
1961	Juraviaska	Russia	-	Immiscible	Carbonate
1962	Adena	Colorado	Propane	Miscible	Sandstone
1964	Hassil-Messaoud	Algeria	Hydrocarbon	Miscible	-
1965	Fairway	Texas	Hydrocarbon	Miscible	Limestone
1968	Ozak-Sual	Russia	Hydrocarbon	Miscible	Sandstone
1970	Goyt-Kart	Russia	Hydrocarbon	Miscible	Sandstone
1972	Kally-Snydor	Texas	CO <sub>2</sub>	Miscible	Carbonate
1972	Levecilland	Texas	CO <sub>2</sub>	Miscible	Limestone
1973	South Swan	Alberta	NGL	Miscible	Carbonate
1976	Flock Creek	West Virginia	CO <sub>2</sub>	Miscible	Sandstone

Table 3.2: Summary of incremental oil recovery of WAG field cases. (Data from Christensen *et al.* SPE International., Mar. 1998.)

Name	Injection pattern	Incremental recovery factor from water flood (%)	Slug size HCPV (%)	WAG ratio
North Pembina	5 spots	9.4	-	-
South Ward	5 spots	3.7		
Kelly Snyder	9 spots	10	1.5	3
South Swan	9 spots	2.0	1	1 to 1.25
Lick Croak	-	3.1	-	1
Slaughter Estate	5 spots	19.6	2.5	2
Fundy-Spinger NE	5 spots	7.5	7.5	2
Wilmington	Line drive	12.5	-	-
Fenn Big Valley	-	15	1.5	1.3
Judy Creek	5 spots	6.5	15	1
Dollarhide	5 spots	19	30	
Wertz lanxiago	-	3.8	2.5	1
N. Ward Esies	5 spots+line	8	1.5	1
Last Soldier field	line	9.9	-	1

The WAG process can be classified in many ways. The most common one is to distinguish between miscible and immiscible WAG displacements:

1. Miscible WAG

This process starts by injecting water then followed by gas slug alternately. Miscibility is a process that composition of the driving and displaced fluid is altered. This happens when light hydrocarbon components of the reservoir oil vaporize and components of injected gas dissolve into the oil phase. It is hard to distinguish between miscible and immiscible WAG processes. A lot of uncertainty is involved in the actual displacement process. Most of the reported miscible projects had to keep reservoir pressure above the minimum miscibility pressure of the fluid. When failing to maintain such a high pressure, loss of miscibility is inevitable. Thus, a real field case may oscillate between miscible and immiscible displacement during the life of production.

2. Immiscible WAG

This process starts by injecting water in a similar manner as the miscible process. The alteration of composition is not achieved in the immiscible WAG process. Therefore, this type of WAG process improves the frontal stability. The use of this type is in the reservoirs with limited gas resources. Sometimes only a small degree of the first gas slug dissolves into the oil. This causes mass exchange at the displacement front. This displacement is called near miscible WAG process.

3. Hybrid WAG

This type of WAG process starts with injectivity of gas instead of water. Then, the first slug is followed by a number of small slugs of water and gas. The field test result is quite similar to miscible WAG process.

4. Simultaneous WAG (SWAG)

This is a process in which water and gas are injected simultaneously. It has been tested in a few reservoirs. It was found that SWAG provides better control of gas mobility than immiscible WAG. However, injecting water and gas simultaneously can result in lower injectivity than single phase injection.

The type of injected gas used in WAG process today can be classified in three groups: CO<sub>2</sub>, hydrocarbon gas, and non-hydrocarbon. Due to the fact that hydrocarbon gas is generally available from the production and for environmental reason, all offshore WAG injections today use hydrocarbon. However, it is not worth to import hydrocarbon gas if it is not available from the production. CO<sub>2</sub> and N<sub>2</sub> miscibility can be obtained by vaporization. CO<sub>2</sub> miscibility is usually achieved at lower pressure than N<sub>2</sub>. Nevertheless, CO<sub>2</sub> is expensive and corrosion problem is inevitable when using CO<sub>2</sub> as an injected gas. Some fields use nitrogen as an injected gas because special supplies are available nearby.

### **3.1.1 Problems in WAG process**

During the production life of an oil field, many operational problems cannot be avoided. In the WAG process, certain problems have been reported from literature and can be summarized as follows:

#### **1. Gas early breakthrough**

Several field cases reported early gas breakthrough due to channeling or override. This problem is considered to be difficult to handle.

#### **2. Reduced injectivity**

Reduced injectivity means that less gas and water can be injected into the reservoir as the WAG process is being carried out. This definitely affects the displacement and oil production. Change in relative permeability is a major cause of reduced injectivity.

#### **3. Corrosion**

Normally, WAG process is conducted as an enhanced oil recovery method. Therefore, the old production facilities are reused. Some of them are not initially designed to operate WAG injection. These problems can be solved by using high quality steel (stainless steel or ferritic steel), coating the pipes, and treating the equipment.

#### **4. Scale formation**

The occurrence of scale in a WAG process is often detected when CO<sub>2</sub> is an injected gas. The scale formation may stress the pipelines and can cause corrosion.

### 3.2 Recovery factor relation

There is a simple equation which helps describe the advantages of WAG process. Oil recovery factor is related to three variables as follows:

$$REC = E_v \cdot E_h \cdot E_m \quad (3.1)$$

where

$REC$  = oil recovery factor

$E_v$  = vertical sweep efficiency

$E_h$  = horizontal sweep efficiency

$E_m$  = microscopic displacement efficiency

The ultimate recovery can be achieved by maximizing each or all of three variables. The contribution of  $E_v$  and  $E_h$  can be considered as macroscopic displacement efficiency.

When miscible displacement occurs, the residual oil will decrease to zero in the flooded zone. Even with an immiscible displacement, the remaining oil saturation after injecting gas is usually lower than the remaining oil saturation after waterflooding. This means that gas flooding has a higher microscopic displacement efficiency than waterflooding.

#### 3.2.1 Horizontal displacement efficiency

The horizontal displacement efficiency ( $E_h$ ) is strongly affected by the frontal stability controlled by mobility ratio which can be defined as:

$$M = \frac{\frac{k_{rg}}{\mu_g}}{\frac{k_{ro}}{\mu_o}} \quad (3.2)$$

If an unfavorable mobility ratio, which means  $M > 1$ , is the case, gas will finger and then cause an early gas breakthrough, decreasing the sweep efficiency.

### 3.2.2 Vertical sweep efficiency

The vertical sweep efficiency ( $E_v$ ) is influenced by the viscous to gravity ratio which can be shown as follows:

$$R_{v/g} = \left( \frac{u\mu_o}{k_o g \Delta\rho} \right) \left( \frac{L}{h} \right) \quad (3.3)$$

where

- $R_{v/g}$  = viscous to gravity ratio
- $u$  = velocity
- $\mu_o$  = oil viscosity
- $L$  = distance between producer and injector
- $k_o$  = permeability to oil
- $g$  = gravity constant
- $\Delta\rho$  = difference of density between the fluids
- $h$  = height of displacement zone.

### 3.3 Reservoir simulation

At present, reservoir simulation is a major tool to quantify or predict the recovery factor in a certain production strategy especially in the enhanced oil recovery process such as WAG injection. Reservoir simulation discretizes the reservoir into a number of grid blocks, and takes into account variation of rock and fluid properties. In this study, the fully implicit method is used to solve for the solutions. This procedure involves simultaneously solving a system of partial differential equations for flow of oil, water, and gas as well as saturation relationship and capillary pressure equations. The flow equation for each grid block can be shown as follows:

For oil phase

$$\frac{\partial}{\partial x} \left( \frac{k_o}{\mu_o B_o} \frac{\partial \Phi_o}{\partial x} \right) + \frac{\partial}{\partial y} \left( \frac{k_o}{\mu_o B_o} \frac{\partial \Phi_o}{\partial y} \right) + \frac{\partial}{\partial z} \left( \frac{k_o}{\mu_o B_o} \frac{\partial \Phi_o}{\partial z} \right) = \frac{\partial}{\partial t} \left( \frac{\phi S_o}{B_o} \right) + \frac{q_{osc}}{V_b} \quad (3.4)$$

For water phase

$$\frac{\partial}{\partial x} \left( \frac{k_w}{\mu_w B_w} \frac{\partial \Phi_w}{\partial x} \right) + \frac{\partial}{\partial y} \left( \frac{k_w}{\mu_w B_w} \frac{\partial \Phi_w}{\partial y} \right) + \frac{\partial}{\partial z} \left( \frac{k_w}{\mu_w B_w} \frac{\partial \Phi_w}{\partial z} \right) = \frac{\partial}{\partial t} \left( \frac{\phi S_w}{B_w} \right) + \frac{q_{wsc}}{V_b} \quad (3.5)$$

For gas phase, both free gas and solution gas are included in flow equation.

$$\begin{aligned} & \frac{\partial}{\partial x} \left( \frac{k_g}{\mu_g B_g} \frac{\partial \Phi_g}{\partial x} \right) + \frac{\partial}{\partial x} \left( \frac{R_s k_o}{\mu_o B_o} \frac{\partial \Phi_o}{\partial x} \right) + \frac{\partial}{\partial y} \left( \frac{k_g}{\mu_g B_g} \frac{\partial \Phi_g}{\partial y} \right) + \frac{\partial}{\partial y} \left( \frac{R_s k_o}{\mu_o B_o} \frac{\partial \Phi_o}{\partial y} \right) + \\ & \frac{\partial}{\partial z} \left( \frac{k_g}{\mu_g B_g} \frac{\partial \Phi_g}{\partial z} \right) + \frac{\partial}{\partial z} \left( \frac{R_s k_o}{\mu_o B_o} \frac{\partial \Phi_o}{\partial z} \right) = \frac{\partial}{\partial t} \left( \frac{\phi S_g}{B_g} \right) + \frac{\partial}{\partial t} \left( \frac{\phi R_s S_o}{B_g} \right) + \frac{q_{gsc}}{V_b} \end{aligned} \quad (3.6)$$

where

- $k_o$  = permeability to oil
- $k_w$  = permeability to water
- $k_g$  = permeability to gas
- $\Phi_o$  = potential at oil phase
- $\Phi_w$  = potential at water phase
- $\Phi_g$  = potential at gas phase
- $B_o$  = oil formation volume factor
- $B_w$  = water formation volume factor
- $B_g$  = gas formation volume factor
- $\mu_o$  = oil viscosity
- $\mu_w$  = water viscosity



$\mu_g$	= gas viscosity
$\phi$	= porosity
$R_s$	= solution gas oil ratio
$S_o$	= oil saturation
$S_w$	= water saturation
$S_g$	= gas saturation
$q_{osc}$	= oil flow rate
$q_{wsc}$	= water flow rate
$q_{gsc}$	= gas flow rate
$V_b$	= grid block bulk volume

The potential terms are defined as follows:

$$\text{For oil} \quad \Phi_o = p_o + \rho_o gh \quad (3.7)$$

$$\text{For gas} \quad \Phi_g = p_g + \rho_g gh \quad (3.8)$$

$$\text{For water} \quad \Phi_w = p_w + \rho_w gh \quad (3.9)$$

where

$\rho_o$  = oil density.

$\rho_g$  = gas density.

$\rho_w$  = water density.

$g$  = gravity constant.

$h$  = height of fluid level.

The saturation equation is expressed as follows:

$$S_o + S_w + S_g = 1 \quad (3.10)$$

The capillary pressure at any point in the system is defined as

$$p_{cow} = p_o - p_w \quad (3.11)$$

$$p_{cog} = p_g - p_o \quad (3.12)$$

where

$p_{cow}$  = capillary pressure for oil-water system

$p_{cog}$  = capillary pressure for oil-gas system

The saturation changes can be expressed in terms of the capillary pressure by using

Chain's rule.

$$\frac{\partial S}{\partial t} = \frac{\partial S}{\partial p_c} \frac{\partial p_c}{\partial t} \quad (3.13)$$

which is rewritten as:

$$\frac{\partial S}{\partial t} = S' \frac{\partial p_c}{\partial t} \quad (3.14)$$

where

$S'$  = inverse of the slope of capillary pressure-saturation curve.

$S'$  can be rewritten in terms of potentials as follows:

$$S' = \frac{\partial S}{\partial p_c} = \frac{S^{n+1} - S^n}{\Phi_o^{n+1} - \Phi_w^n} \quad (3.15)$$

where

$n$  = time index

$i$  = spatial index

From the relation of capillary pressure and saturation above, Eq. 3.4 can be rearranged to the finite difference forms as follows:

$$\begin{aligned} & \frac{I}{\Delta x} \left[ \left( \frac{k_o}{\mu_o} \right)_{i+\frac{1}{2}} \left( \frac{\Phi_{oi}^{n+1} - \Phi_{oi}^{n+1}}{\Delta x} \right) - \left( \frac{k_o}{\mu_o} \right)_{i-\frac{1}{2}} \left( \frac{\Phi_{oi}^{n+1} - \Phi_{oi-1}^{n+1}}{\Delta x} \right) \right] \\ & = - \frac{\Phi S'}{\Delta t} \left[ (\Phi_{oi}^{n+1} - \Phi_{oi}^n) - (\Phi_{wi}^{n+1} - \Phi_{wi}^n) \right] \end{aligned} \quad (3.16)$$

Note that Eq. 3.16 shows the finite difference form of the flow of oil in the x direction only.

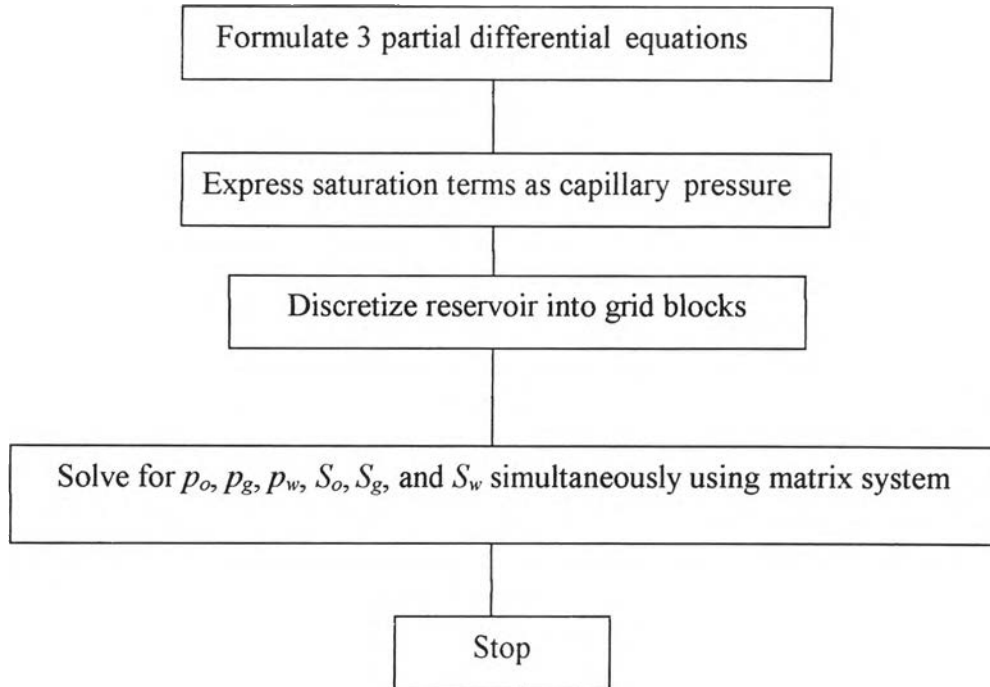


Figure 3.1: Procedure of the fully implicit solution method.

Figure 3.1 shows the calculation flow chart of fully implicit solution procedure. First, the differential flow equations of oil water and gas are formulated. Then the reservoir is discretized into grid blocks. By using a matrix system for the finite difference forms, the pressures and saturations of oil, water and gas are solved implicitly. Then, the new capillary pressure is obtained. From the relation of capillary pressure-saturation, the saturation of each phase can also obtained.

Reservoir simulation can be classified into black oil and compositional simulations. The black oil model can handle reservoirs in which the fluid has the following characteristics:

1. The hydrocarbon composition does not largely change when gas is liberated.
2. The state of fluid should be far from the critical point.
3. The production scenario is isothermal.

Beside the characteristics mentioned above, the commercial black oil reservoir simulation used in this study has Larsen and Skauge relative permeability hysteresis that was constructed directly for the WAG process.

Another type of simulation is compositional reservoir simulation. It is required when there is a significant change of composition. The computation of flow equations for each grid block is conducted by using material balance for each component. Additional computational time is required for iterative solving of cubic equation of state for each component. Practically, flow calculations and equation of state calculation require less than 50% of CPU time of compositional simulation while the rest is required for flash and equation of state calculation.

For compositional reservoir simulation, the composition exchange in the x direction can be described by an equation as follows:

$$\frac{\partial}{\partial x} \left[ \sum_{i=1}^3 c_{ij} \frac{k_i}{\mu_i} \rho_i \frac{\partial P_i}{\partial x} \right] = \frac{\partial}{\partial t} \left[ \sum_{i=1}^3 \phi S_i \rho_i c_{ij} \right] + \sum_{i=1}^3 q_i \alpha_{ij} \quad (3.17)$$

- where  $c_{ij}$  = mass fraction of component  $j$  in  $i$  phase  
 $i$  = phase index (oil, gas and water)  
 $j$  = component index (1, 2, 3 ...n)  
 $\rho_i$  = density of  $i$  phase  
 $\alpha_{ij}$  = mass fraction of component  $j$  in  $i$  phase for sink/source term

### 3.3.1 Peng-Robinson Equation of state

In this study, Peng-Robinson equation of state is used in the compositional reservoir model. Modified from Van der Waals equation, Peng and Robinson (1965) equation developed a slight change in molecular attraction term as follows.

$$\left[ p + \frac{a_T}{V_M (V_M + b) + b(V_M - b)} \right] (V_M - b) = RT \quad (3.18)$$

where

- $R$  = gas constant  
 $T$  = temperature  
 $V_M$  = molar volume

$$a_T = a_c \alpha \quad (3.19)$$

$$\alpha_c = 0.45724 \frac{R^2 T_c^2}{p_c} \quad (3.20)$$

$$b = 0.07780 \frac{RT_c}{p_c} \quad (3.21)$$

$$\alpha^{\frac{1}{2}} = 1 + m(1 - T_r^{\frac{1}{2}}) \quad (3.22)$$

$$m = 0.37464 + 1.54226\omega - 0.26992\omega^2 \quad (3.23)$$

Note that term  $\frac{a_T}{V_M(V_M + b) + b(V_M - b)}$  represents the correction pressure for

the force of attraction between the molecules. Constant  $b$  is the correction to the molar volume due to the volume occupied by the molecules.

### Mixing Rules

When the system contains several components, the following mixing rules are used with Peng-Robinson equation of state.

$$a = \sum_i \sum_j y_i y_j a_{ij} \quad (3.24)$$

and

$$b = \sum_j y_j b_j \quad (3.25)$$

where

$$a_{ij} = (1 - \delta_{ij})(a_i a_j)^{\frac{1}{2}} \quad (3.26)$$

Thus,

$$a = \sum_i \sum_j y_i y_j (a_i a_j)^{\frac{1}{2}} (1 - \delta_{ij}) \quad (3.27)$$

The terms  $\delta_{ij}$  are binary interaction coefficients, which are assumed to be independent of pressure and temperature. Values of the binary interaction coefficients can be obtained by fitting the equation of state to gas-liquid equilibrium data for each binary mixture.

$$a_j = \Omega_a(T, j) \frac{P_j}{T_j^2} \quad (3.28)$$

$$b_j = \Omega_b(T, j) \frac{P_{\eta}}{T_{\eta}} \quad (3.29)$$

$$\Omega_a(T, j) = \Omega_{a_0} \left[ 1 + (0.37464 + 1.54226\omega_j - 0.26992\omega_j^2) \left( 1 - T_{\eta}^{-\frac{1}{2}} \right) \right]^2 \quad (3.30)$$

$$\Omega_b(T, j) = \Omega_{b_0} \quad (3.31)$$

where

$$\Omega_{a_0} = 0.457235$$

$$\Omega_{b_0} = 0.07796$$

### 3.3.2 Flash calculation

For compositional reservoir model, the equilibrium constant for each component can be defined as follows:

$$K_i = \frac{y_i}{x_i} \quad (3.32)$$

At bubble point pressure

$$\sum_{i=1}^N z_i K_i = 1 \quad (3.33)$$

At dew point pressure

$$\sum_{i=1}^N \frac{z_i}{K_i} = 1 \quad (3.34)$$

where  $z_i$  = mole fraction of feed component  $i$

$x_i$  = mole fraction of component  $i$  in the liquid phase

$y_i$  = mole fraction of component  $i$  in the vapor phase

Note that in compositional reservoir model, the equilibrium constant can be calculated using Wilson equation as stated below:

$$K_i = \frac{\exp \left[ 5.37(1 - \omega_i) \left( 1 - \frac{1}{T_n} \right) \right]}{p_n} \quad (3.35)$$

where

$p_{ri}$  = pseudoreduced pressure of the component.

$T_{ri}$  = pseudoreduced temperature of the component.

### 3.4 Relative permeability hysteresis model

As mentioned earlier that there is a change in the relative permeability curves between the drainage and imbibition process during a WAG process. In this study, two relative permeability hysteresis model is considered.

#### 3.4.1 Killough model

The first model to be used was developed by Killough (1976). It considers gas as a non-wetting phase. As shown in Figure 3.2, line 1 - 2 represents the primary drainage relative permeability curve. Line 2 - 3 represents the primary imbibition relative permeability curve. These two curves meet at point 2, which is the point that the non-wetting phase relative permeability is maximum. During the WAG process, if there is an oscillation in saturation which causes a switch between drainage and imbibition process, the relative permeability value will not be taken from the previous curve but will be read from an intermediate scanning curve (line 4 - 5 in Figure 3.2). After following the scanning curve, if further drainage process occurs, the relative permeability will retrace along the scanning curve until the maximum non-wetting phase saturation ( $S_{hy}$ ) is reached.

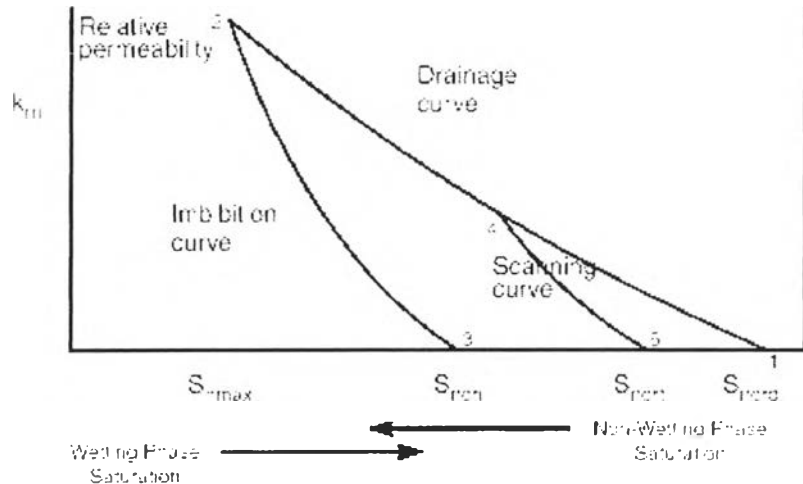


Figure 3.2: Killough model for non-wetting phase hysteresis.

In Killough model, the trapped critical saturation can be calculated as

$$S_{ncrt} = S_{ncrd} + \frac{S_{hy} - S_{ncrd}}{A + C(S_{hy} - S_{ncrd})} \quad (3.36)$$

$$A = 1 + a(S_{n\max} - S_{hy}) \quad (3.37)$$

$$C = \frac{1}{S_{ncr} - S_{ncrd}} - \frac{1}{S_{n\max} - S_{ncrd}} \quad (3.38)$$

The relative permeability corresponding to the non-wetting phase ( $S_n$ ) on the scanning curve can be calculated by

$$k_{rn}(S_n) = \frac{k_{rmi}(S_{norm})k_{rmd}(S_{hy})}{k_{rmd}(S_{n\max})} \quad (3.39)$$

$$S_{norm} = S_{ncr} + \frac{(S_n - S_{ncr})(S_{n\max} - S_{ncr})}{S_{hy} - S_{ncr}} \quad (3.40)$$

where  $k_{rmi}$  and  $k_{rmd}$  = the relative permeability on the bounding imbibition and drainage process, respectively.

$C$  = Land 's constant.

$S_{ncr}$  = trapped critical saturation of non-wetting phase.

$S_{ncr}$  = end point saturation of non-wetting phase in imbibition process.

$S_{ncrd}$  = end point saturation of non-wetting phase in drainage process.

$a$  = a parameter input to the simulation and defaults to 0.1.

### 3.4.2 Larsen and Skauge model

The second relative permeability hysteresis model to be used in this study was developed by Larsen and Skauge (1998). This model was specifically designed for a WAG process. The model is an extension of the Killough (1976) model.

#### 3.4.2.1 Hysteresis of gas relative permeability

The Larsen and Skauge model takes saturation history into account by making the gas and water relative permeabilities dependent on two phase saturations and making the trapped gas saturation history dependent on hysteresis loop or cycle of alternation as shown in Figure 3.3. Figure 3.4 shows the construction of secondary drainage curve. First, a line that is at best parallel to the primary drainage curve is drawn. This parallel line starts at the end of primary imbibition curve. The actual secondary drainage curve is constructed by damping the gas relative permeability



curve by a factor which depends on water saturation at the beginning of the drainage phase( $S_w^f$ ).

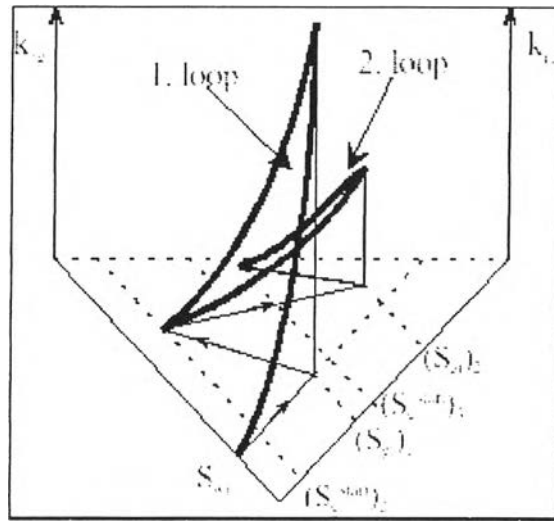


Figure 3.3: Larsen and Skauge gas hysteresis (3D projection).

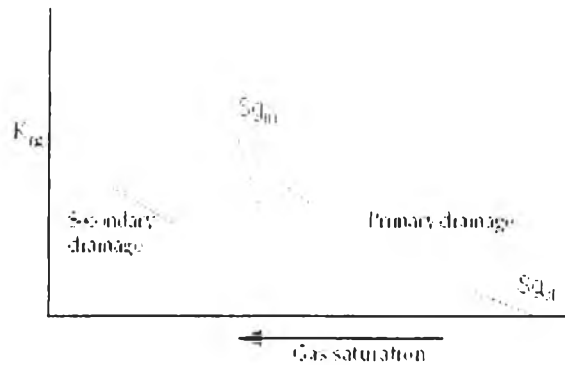


Figure 3.4: Larsen and Skauge hysteresis (2D projection).

The equation for secondary drainage gas relative permeability is

$$k_{rg}^{drain,n} = \left[ (k_{rg}^{input}(S_g) - k_{rg}^{input}(S_g^{start})) \cdot \left( \frac{S_w}{S_w^f} \right)^\alpha \right]^n + k_{rg}^{imb,(n-1)}(S_g^{start}) \quad (3.41)$$

where

$k_{rg}^{drain,n}$  = calculated secondary drainage relative permeability as a function of  $S_g$

$k_{rg}^{input}$  = input relative permeability at  $S_g$

$k_{rg}^{input}(S_g^{start})$  = input relative permeability at the gas saturation at the start of the secondary drainage curve

$S_{wco}$  = connate water saturation

$S_{wstart}$  = water saturation at the start at the secondary drainage curve

$k_{rg}^{imb}(S_g^{start})$  = relative permeability at the start of secondary drainage curve

$\alpha$  = reduction exponent

Thus, there will be a tendency for the gas relative permeability to decrease in successive injection cycles if the water saturation at the beginning of each cycle increases.

During secondary imbibition (decreasing gas saturation), the gas relative permeability curve equals to the relative permeability of secondary drainage curve at a transformed saturation as follows:

$$k_{rg}^{imb,n}(S_g) = k_{rg}^{drain,n}(S_{gf}^{trans}) \quad (3.42)$$

where  $n$  is the number of hysteresis loop and

$$S_{gf} = \frac{1}{2} \cdot \left[ (S_g - S_{gr}) + \sqrt{(S_g - S_{gr})^2 + \frac{4}{C^{trans}} \cdot (S_g - S_{gr})} \right] \quad (3.43)$$

$$S_{gf}^{trans} = S_{gf} + S_g^{end} \quad (3.44)$$

$$\frac{1}{S_{gr} - S_g^{end}} - \frac{1}{S_{gi} - S_g^{end}} = C^{trans} \quad (3.45)$$

where

$S_{gi}$  = initial gas saturation

$S_{gf}$  = free gas saturation.

$S_{gr}$  = the residual (trapped) gas saturation.

$S_g$  = gas saturation.

$S_g^{end}$  = gas saturation at the end of the imbibition curve.

superscript

trans = transformed

### 3.4.2.2 Hysteresis of water relative permeability

For the water phase, the model is based on an observation that water relative permeability measuring after gas flooding has apparently less mobility. In this water hysteresis model, two relative permeability curves must be input. One is the ‘normal’ input (the 2-phase curve), the other is measured with three phases present (the 3-phase curve). The water relative permeability is then constructed as an interpolation between these curves, dependent on the gas saturation at the start of the hysteresis loop as shown in Figure 3.5.

During imbibition, the relative permeability function is shown as follows:

$$k_{rw}^{imb} = k_{rw2} \cdot \left(1 - \frac{S_g^{start}}{S_{gmax}}\right) + k_{rw3} \cdot \left(\frac{S_g^{start}}{S_{gmax}}\right) \quad (3.45)$$

where

$k_{rw}^{imb}$  = calculated imbibition relative permeability

$k_{rw2}$  = 2-phase relative permeability at  $S_w$

$k_{rw3}$  = 3-phase relative permeability at  $S_w$

$S_{gmax}$  = maximum attainable gas saturation,  $1 - S_{wco} - S_{ogcr}$

$S_{wco}$  = connate water saturation

$S_{ogcr}$  = critical oil to gas saturation

During drainage, the relative permeability function is shown as follows:

If  $S_g > S_g^{drain}$ , then

$$k_{rw}^{drain} = k_{rw}^{imb} \cdot \left(1 - \frac{S_g - S_g^{drain}}{S_{gmax} - S_g^{drain}}\right) + k_{rw3} \cdot \left(\frac{S_g - S_g^{drain}}{S_{gmax} - S_g^{drain}}\right) \quad (3.46)$$

If  $S_g < S_g^{drain}$ , then

$$k_{rw}^{drain} = k_{rw}^{imb} \cdot \left(1 - \frac{S_g^{drain} - S_g}{S_g^{drain}}\right) + k_{rw2} \cdot \left(\frac{S_g^{drain} - S_g}{S_g^{drain}}\right) \quad (3.47)$$

where

$S_g^{drain}$  = gas saturation at the start of the drainage process

$k_{rw}^{drain}$  = calculated drainage curve

Since there is no fluctuation in the oil saturation, hysteresis cannot be taken into account in the oil phase. The residual oil saturation is made dependent on the trapped gas saturation, introducing the constant  $\alpha$  as follows:

$$S_{ro} = S_{om} - \alpha \cdot S_{gt} \quad (3.48)$$

where

$S_{om}$  = minimum residual oil saturation.

$S_{gt}$  = trapped gas saturation

$\alpha$  = input constant which can vary between 0 and 1. If the construction from the trapped gas saturation ( $\alpha S_{gt}$ ) exceeds  $S_{om}$ , the residual oil saturation is set to 0.

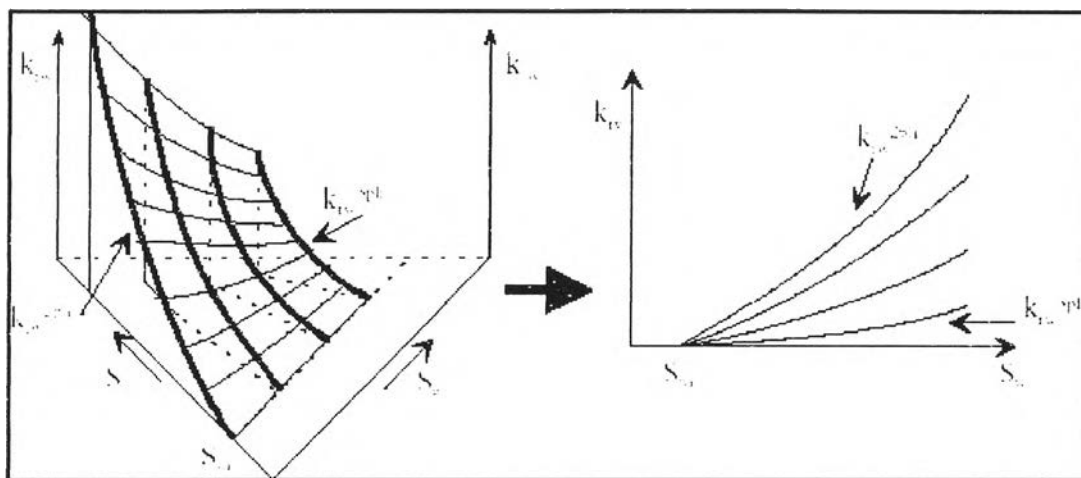


Figure 3.5: Water relative permeability hysteresis.

Due to the fact that Larsen and Skauge hysteresis model is available in black oil reservoir simulation only, the optimization of WAG process conducted on both black oil and compositional reservoir model will use Killough relative permeability hysteresis model. The effect of Larsen and Skauge model is investigated separately.

### 3.5 Parametric study

There are many parameters that affect the WAG injection. In this study, parameters which are water-gas ratio and slug sizes will be optimized with varied horizontal permeabilities ( $k_h$ ), vertical to horizontal permeability ratios ( $k_v/k_h$ ) and position of injector and producer.

#### 3.5.1 Water-gas ratio

Many studies have shown that improvement of sweep efficiency of the WAG injection can be achieved by supplying gas to the gas/water front at a rate corresponding to the volume of gas trapped by the advancing water. Gas bank ahead of the front enables another gas bank to reduce residual oil. Therefore, optimization of water gas ratio will directly enhance the WAG process. Blackwell (1960) suggested the following equation to calculate minimum gas-water ratio for Brent reservoir in the North sea.

$$\frac{Q_g}{Q_w} = \frac{1}{H} \sum_{i=1}^n h_i \left[ \frac{(1 - S_{w,rg} - S_{orm})}{(S_{w,rg} - S_{wc} - S_{ww})_i} - \left( \frac{k_{w,rg}}{k_{g,wr}} \right)_i \left( \frac{\mu_g}{\mu_w} \right)_i (1 - S_{wc} - S_{orm} + S_{ww}) \right] \quad (3.49)$$

where

$$S_{w,rg} = 1 - S_{gtr} - S_{orm}$$

$$S_{gtr} = \frac{S_{gi}}{(1 + cS_{gi})}$$

$S_{orm}$  = three phase residual oil saturation

$S_{wc}$  = water connate saturation

$S_{gtr}$  = trapped gas saturation

$S_{gi}$  = initial gas saturation

$C$  = Land's constant

$k_{w,rg}$  = relative permeability of water to gas flow evaluated at  $S_{w,rg}$

$k_{g,wr}$  = relative permeability of gas to water flow evaluated at  $S_{w,rg}$

$\mu_g$  = gas viscosity

$\mu_w$  = water viscosity

$S_g$  =  $1 - S_{orm} - S_{wc}$

$H$  = reservoir thickness.

$h_i$  = thickness of the  $i^{\text{th}}$  layer.

The Blackwell equation calculates the minimum gas-water ratio at which the process can be considered as WAG injection. If the gas-water ratio is less than the minimum value, the process will simply be considered as waterflooding. And practically, an excess volume of gas is required to proceed the water bank to reduce the residual oil saturation. For this reason, we should consider water-gas ratio as an important parameter that will be optimized to achieve the optimal results from WAG injection.

### 3.5.2 Slug size or cycle size

The slug size is the time period to complete a full cycle of injection. It is a period of gas injection followed by another period of water injection. Segregated flow which decreases the injection efficiency can occur if gas is injected in high volume. This can lead to gas overriding and early breakthrough. On the other hand, water can override oil, leading to water under-riding. Surguchev(1992) suggested that the optimization of WAG process could be reached if water and gas flow in the reservoir at the same speed. But this can occur only in a short period due to the difference between viscosities and densities of water and gas. Therefore, slug size is another significant parameter that need to be optimized .